Cell Reports, Volume *34*

Supplemental Information

NAD^+ boosting reduces age-associated amyloidosis and restores mitochondrial homeostasis in muscle

Mario Romani, Vincenzo Sorrentino, Chang-Myung Oh, Hao Li, Tanes Imamura de Lima, Hongbo Zhang, Minho Shong, and Johan Auwerx

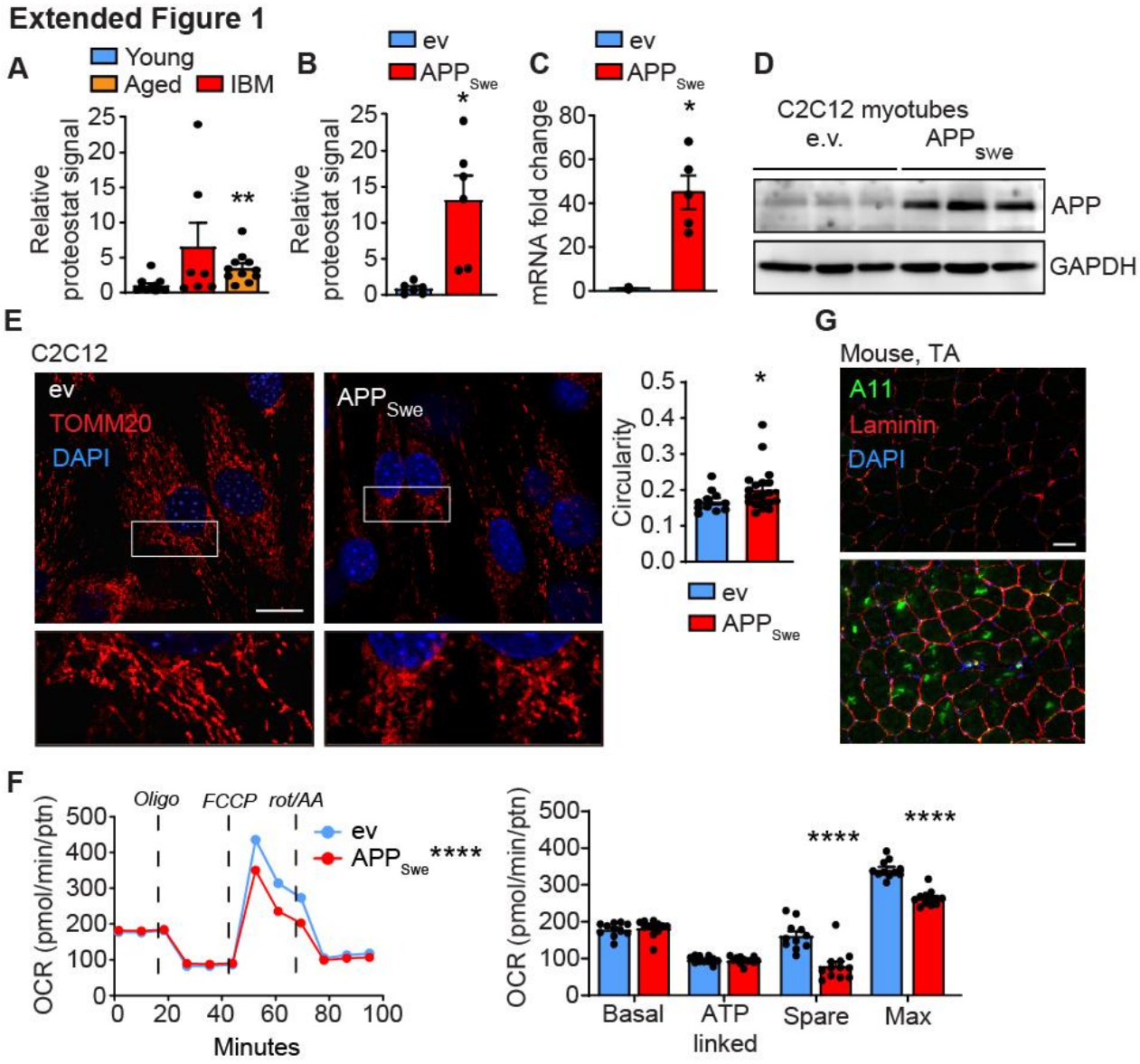

Extended Figure 1. Proteostasis and mitochondrial alterations during aging and proteotoxic stress in muscle cells (related to Figure 2). a-b, Proteostat signal quantification normalized over the number of cells for experiments shown in **Figure 1a-b** (Young *n=11*, aged *n=7*, IBM *n=11*; C2C12 *n=6*). **c-d,** qRT-PCR RNA analysis (*n*=5 biological replicates) **(c)** and APP immunoblotting (*n*=3 biological replicates) **(d)** of control and APP_{Swe}-expressing C2C12 myotubes. **e**, Confocal images of control and APP_{Swe}-expressing C2C12 myotubes, stained using a TOMM20 antibody to reveal the mitochondrial network and relative circularity assessment (in which 1 represents a perfect circle and 0 a line) (scale bar, 50µm). **f**, Oxygen consumption rates in C2C12ev or APP_{Swe}-expressing C2C12 myoblasts treated with oligomycin (Oligo), FCCP and rotenone/antimycin A (Rot-AA). Error bars represent the mean ± SEM. **e**, Representative images of immunostainings of laminin and A11

positive deposits in Tibialis anterior (TA) muscles of young (3 months) or aged (24 months) male C57BL/6J mice. All experiments were performed independently at least twice. See **Methods** for further details. Values in the figure are mean ± s.e.m. **P*<0.05; *****P*≤0.0001.. For all the individual p values, see the **Excel data source Extended Fig. 1.**

Extended Figure 2

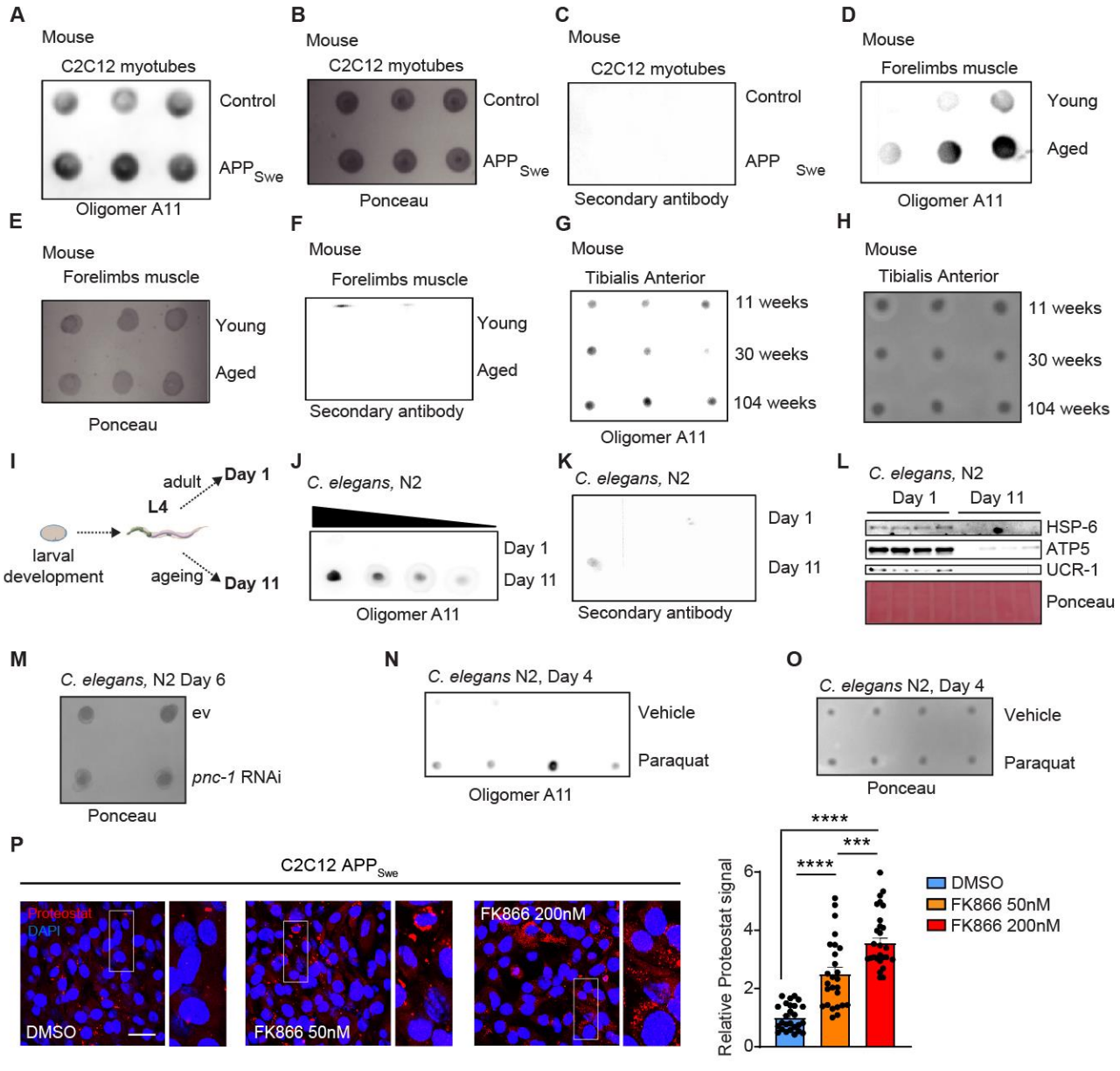

Extended Figure 2. Dot blotting to detect amyloid-like deposits in mouse muscle and in *C. elegans* (related to Figure 2). a,d,g, Dot blot analyses based on A11 antibody detection of protein lysates from control and APP_{Swe}-expressing C2C12 myotubes (**a**, *n*=3 biological replicates per group), young (3 months) and old (24 months) male C57BL/6J mice (**d**, *n*=3 mice per group) and

11, 30 or 104 weeks old male C57BL/6J mice (**g**, *n*=3 mice per group). Relative quantification of the blot intensities is reported in **Extended Data Table 5**. **b,e,h,** Ponceau staining, as a loading control, of the membranes loaded with protein lysates from control and APP_{Swe}-expressing C2C12 cells (**b**, *n*=3 biological replicates per group), young and old mice (**e**, *n*=3 mice per group), and 11, 30 or 104 weeks old mice(**h**, *n*=3 mice per group). These blots correspond to **a**, **d** and **h**. **c,f,** Control experiment for the dot blotting analysis of the same samples as in **a** and **d**, using only the secondary antibody. **i,** Schematic for the *C. elegans* experimental observations in **Figure 2e,g,h,i** and **Extended Figure 2 j,k,m** using young (day 1) and aged (day 11) N2 worms. **j,** Serial dilutions of 1 biological sample from young (day 1) and aged (day 11) N2 worms, showing the specificity of detection of the A11 antibody in worm protein lysates. **k,** Control experiment for the dot blotting analysis of the samples in **Figure 2k**, using only the secondary antibody. **l,** Immunoblot of the mitochondrial proteins HSP-6, ATP5 and UCR-1 from young and old N2 worms. **m,** Ponceau staining, as a loading control, of the membrane loaded with protein lysates from **Figure 2i**. **n-o,** A11 dot blotting of N2 (day 4) worms treated with paraquat (50uM) (n=4 biological replicates per group) and relative ponceau staining. Relative quantification of the blot intensities is reported in **Supplementary Table 5**. **p,** Representative confocal images and relative quantification of APP_{Swe}-expressing C2C12 myoblasts (scale bar, 10μm) treated with FK866 (50 or 200nM) and stained with the Proteostat fluorescent dye. All experiments were performed independently twice. Values in the figure are mean ± s.e.m. ***$P \leq 0.001$; ****$P \leq 0.0001$. For all the individual p values, see the **Excel data source Extended Fig. 2**.

Extended Figure 3

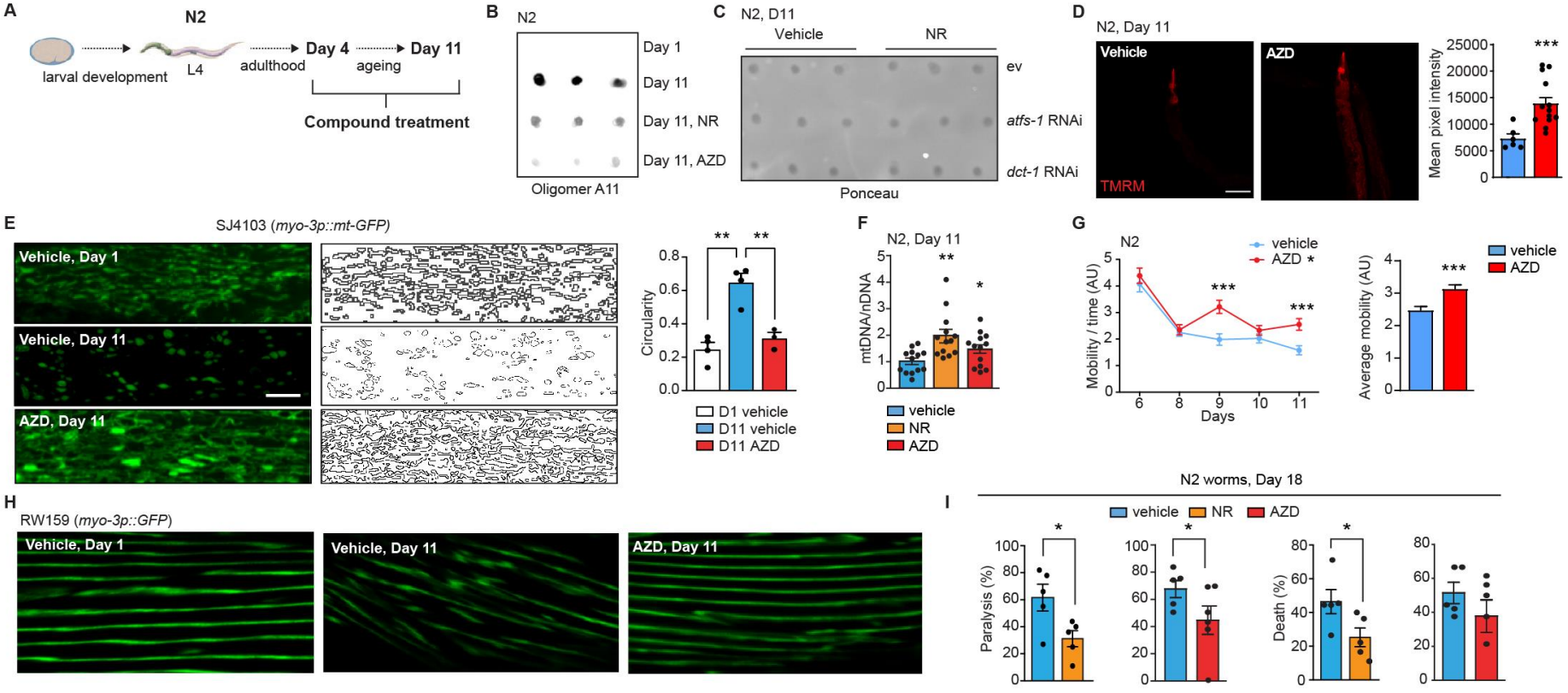

Extended Figure 3. AZD treatment improves mitochondrial and fitness parameters in aged *C. elegans* (related to Figure 3). a, Scheme of the experimental design including compound interventions during aging in N2 worms. **b**, A11 dot blotting of young (day 1) and aged (day 11) N2 worms treated as indicated in **a**, with NR (1mM) and a PARP inhibitor (AZD; 300nM) (*n*=3 biological replicates per group). Day 1 and day 11 samples are the same as **Fig 2e**. Relative quantification of the blot intensities is reported in **Supplementary Table 5**. **c**, Ponceau staining, as a loading control, of the membrane loaded with protein lysates from **Figure 3b**. **d**, Confocal images of TMRM staining of aged (day 11) N2 worms treated as indicated in **Extended Fig 3a**, with AZD (300uM) (Vehicle, n=6; AZD, n=13 worms) and relative quantification. Scale bar, 100µm. **e**, Confocal images of mitochondrial networks and corresponding morphology analyses including mitochondria outline and circularity assessment (in which 1 represents a perfect circle and 0 a line) in young (day 1) and aged (day 11) SJ4103 (*myo-3p::mt-GFP*) worms treated with AZD (300 nM) following the experimental pipeline shown in **Fig. 3a** (D1, *n*=3; D11, *n*=4; D11 AZD, *n*=3). Scale bar, 10µm. **f**, mtDNA/nDNA ratio in N2 worms treated with NR (1mM) and AZD (300 nM) (*n*=13 animals per group). **g**, Spontaneous mobility and average mobility of N2 worms treated with vehicle or AZD (300 nM) as in **a** (vehicle, *n*=70; AZD, *n*=80 worms). Overall differences between conditions were assessed by two-way ANOVA (Average mobility); differences between conditions at individual time points were assessed using post hoc Sidak's multiple comparison test. **h**, Confocal images of GFP-labeled muscle fibers in young (day 1) and aged (day 11) RAW1596 (*myo-3p::GFP*) worms treated with AZD (300 nM) as in **a** (*n*=20 per group). Scale bar, 10µm. **i**, Percentage of paralyzed and dead D18 N2 worms after vehicle or AZD treatment (*n*=5 biological replicates). See **Methods** for further details. Values in the figure are mean ± s.e.m. **P*<0.05; ***P*≤0.01; ****P*≤0.001. Differences for two groups were assessed using two-tailed *t* tests (95% confidence interval) in panel **a**, **b**, **d**, and **e**. All experiments were performed independently at least twice. AU, arbitrary units. For all the individual p values, see the **Excel data source Extended Fig. 3**.

Extended Figure 4

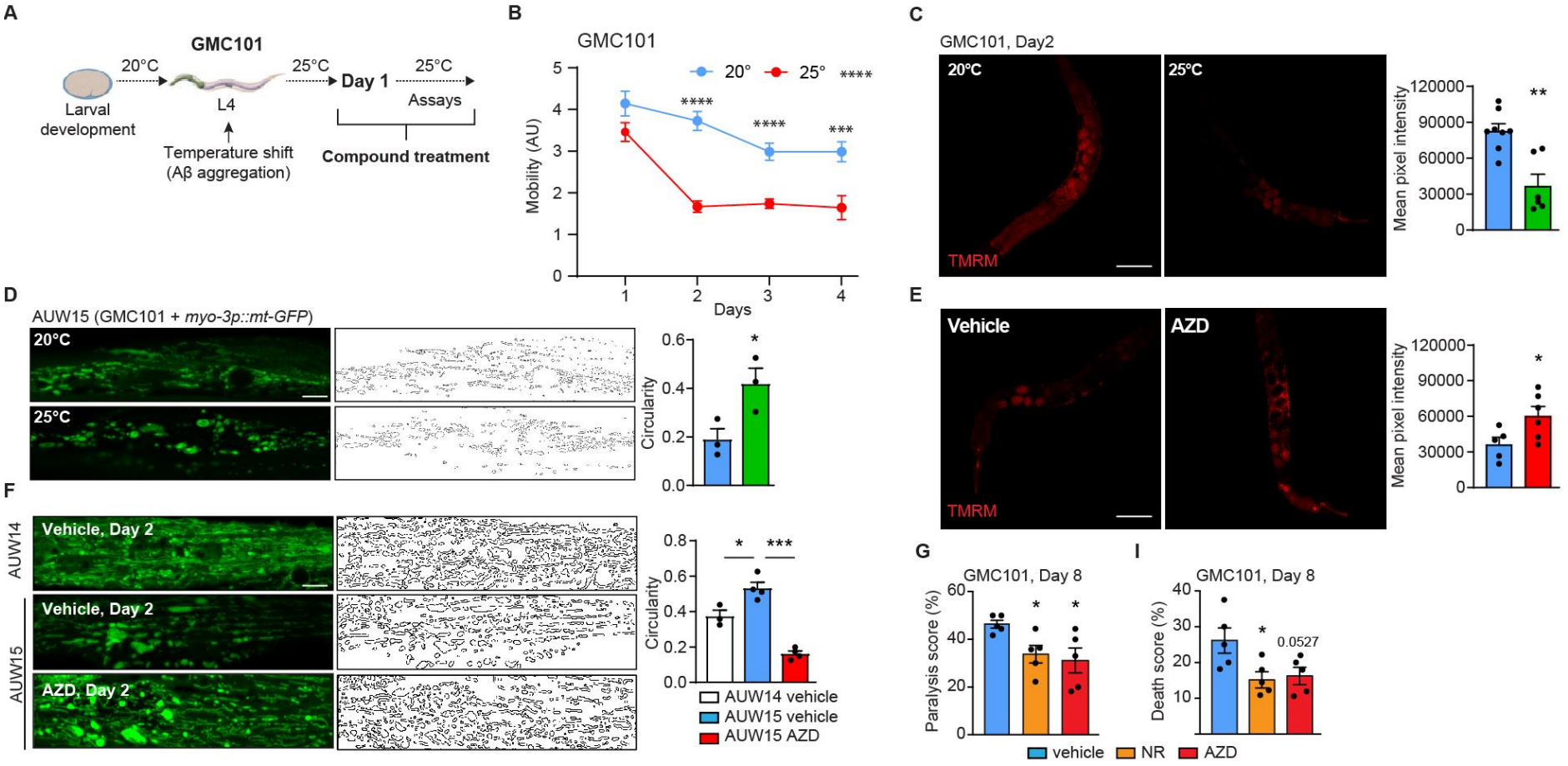

Extended Figure 4. AZD beneficially impacts on Aβ -associated mitochondrial dysfunction in *C.elegans* (related to Figure 5). a, Scheme of the experimental design including activation of Aβ-aggregation and compound interventions in GMC101 worms. **b**, Spontaneous mobility of GMC101 worms cultured at 20° or 25°C as in **a** (20°C, *n*=46; 25°C, *n*=43 worms). Overall differences between conditions were assessed by two-way ANOVA; differences between conditions at individual time points were assessed using post hoc Sidak's multiple comparison test. **c**, Confocal images of TMRM staining of day 2 GMC101 worms cultured at 20° or 25°C (20°C, *n*=8; 25°C, *n*=6 worms) and relative quantification. Scale bar, 100µm. **d**, Confocal images of mitochondrial networks and corresponding morphology analyses including mitochondria outline and circularity assessment (in which 1 represents a perfect circle and 0 a line) in Day 2 AUW15 (GMC101 + *myo-3p::mt-GFP*) worms cultured at 20° or 25°C (*n*=3 per group). Scale bar, 10µm. **e**, Confocal images of TMRM staining of day 2 GMC101 worms cultured at 25°C and treated with AZD (300nM) as in **a** (Vehicle, n=5; AZD, n=6 worms) and relative quantification. Scale bar, 100µm. **f**, Confocal images of mitochondrial networks and corresponding morphology analyses including mitochondria outline and circularity assessment (in which 1 represents a perfect circle and 0 a line) in Day 2 AUW14 (CL2122 + *myo-3p::mt-GFP*) and AUW15 (GMC101 + *myo-3p::mt-GFP*) worms cultured at 25°C and treated with AZD (300nM) as in **a** (AUW14, *n*=3; AUW15 Vehicle, *n*=4; AUW15 AZD, *n*=4 worms). Scale bar, 10µm. **g-h**, Percentage of paralyzed (**f**) and dead (**g**) D8 GMC101 worms after compound treatment (*n*=5 biological replicates). For all the individual p values, see the **Excel data source Extended Fig. 3**. Values in the figure are mean ± s.e.m. **P*<0.05; ***P*≤0.01; ****P*≤0.001; *****P*≤0.0001.

Extended Figure 5

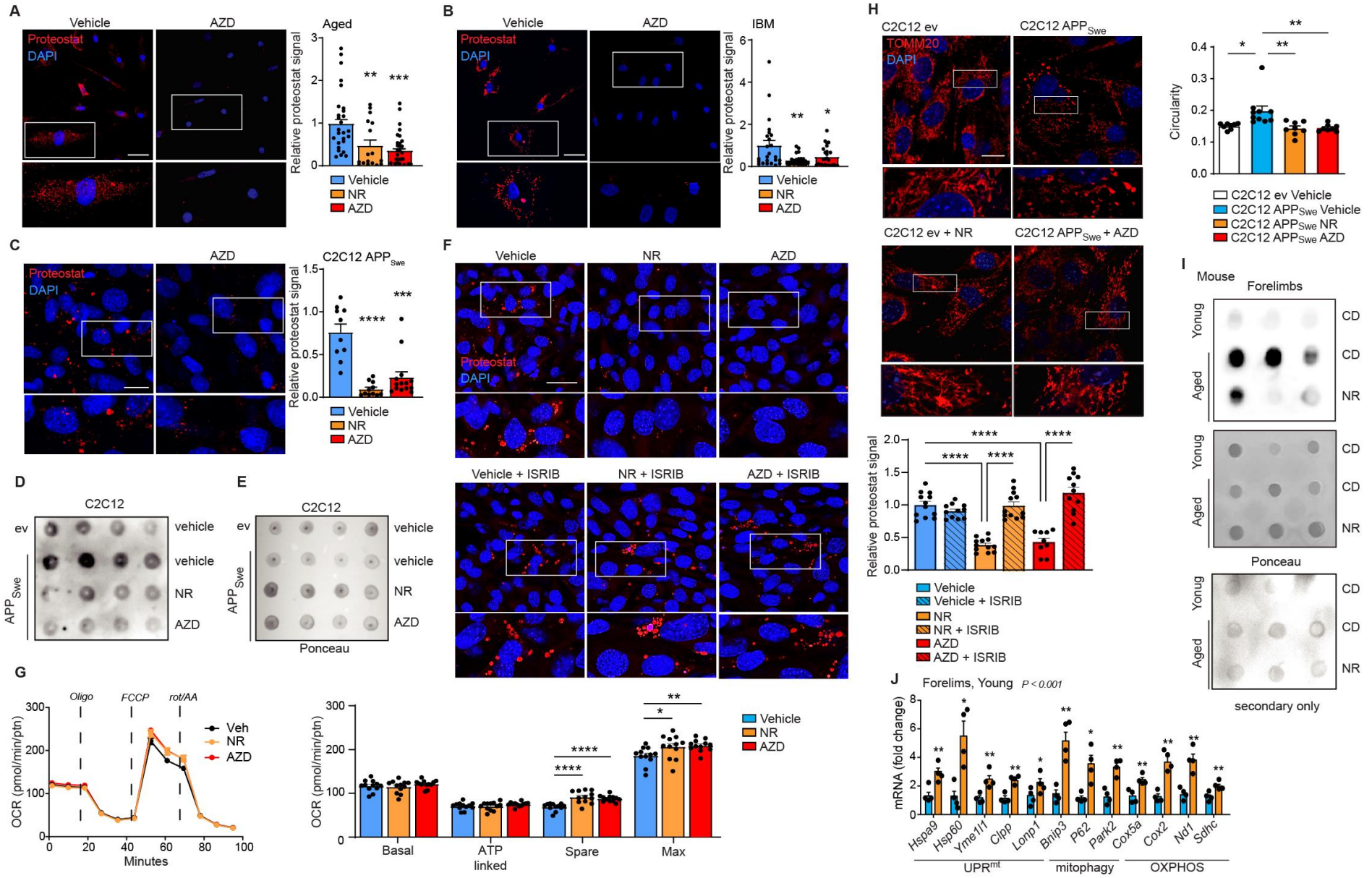

Extended Figure 5. NAD^+ boosting interventions and their effects on proteostasis and mitochondria in cells and in vivo (related to Figure 6). a-c, Representative confocal images of primary human muscle cells from an aged and an IBM donor, (scale bar, 50µm) (**a,b**), or APP_{Swe}-expressing C2C12 myotubes (scale bar, 10µm) (**c**) treated with AZD (1uM) and stained with the Proteostat fluorescent dye and relative Proteostat signal quantification normalized on the number of cells for experiments shown in **Figure 5a-c** (Aged+vehicle *n=34*, aged+NR *n=17*, aged+AZD *n=33*; IBM+vehicle *n=25*, IBM+NR *n=25*, IBM+AZD *n=31*; C2C12+Vehicle *n=11*, C2C12+NR *n=11*, C2C12+AZD *n=14*). **d,e**, A11 dot blot analyses of protein lysates from APP_{Swe}-expressing C2C12 myotubes (*n*=4 biological replicates per group) after compound treatment (NR, 3mM; AZD, 1uM) and relative ponceau control. Relative quantification of the blot intensities is reported in **Extended Data Table 5**. **f**, Representative confocal images of APP_{Swe}-expressing C2C12 myoblast (scale bar, 10µm) treated with NR (1mM), AZD (1uM), and ISRIB (0,5uM) and stained with the Proteostat fluorescent dye and relative Proteostat signal quantification normalized on the number of cells (Vehicle *n=13*, Vehicle + ISRIB *n=11*, NR *n=12*, NR + ISRIB *n=12*, AZD *n=9*, AZD + ISRIB *n=11*). **g**, Oxygen consumption rates in C2C12ev or APP_{Swe}-expressing C2C12 myoblasts treated with NR (3mM) or AZD (1uM) and oligomycin (Oligo), FCCP and rotenone/antimycin A (Rot-AA). Error bars represent the mean ± SEM. **h**, Representative confocal images of control and APP_{Swe}-expressing C2C12 myotubes and corresponding morphology analyses including mitochondria outline and circularity assessment (in which 1 represents a perfect circle and 0 a line) after compound treatment (NR, 3mM; AZD, 1uM), stained using a TOMM20 antibody to reveal the mitochondrial network (scale bar, 50µm). **i**, A11 dot blot analyses and relative controls of protein lysates from young (3 months) and old (24 months) male C57BL/6J mice (*n*=3 mice per group) in control conditions and after compound treatment (NR, 3mM). Relative quantification of the blot intensities is reported in **Extended Data Table 5**. **l**, MSR transcript analysis of forelimbs muscles of young male mice C57BL/6J following NR treatment (*n*=4 animals). For all the individual p values, see the **Excel data source Extended Fig. 5.** Values in the figure are mean ± s.e.m. **P*<0.05; ***P*≤0.01; ****P*≤0.001; *****P*≤0.0001.

Extended Figure 6

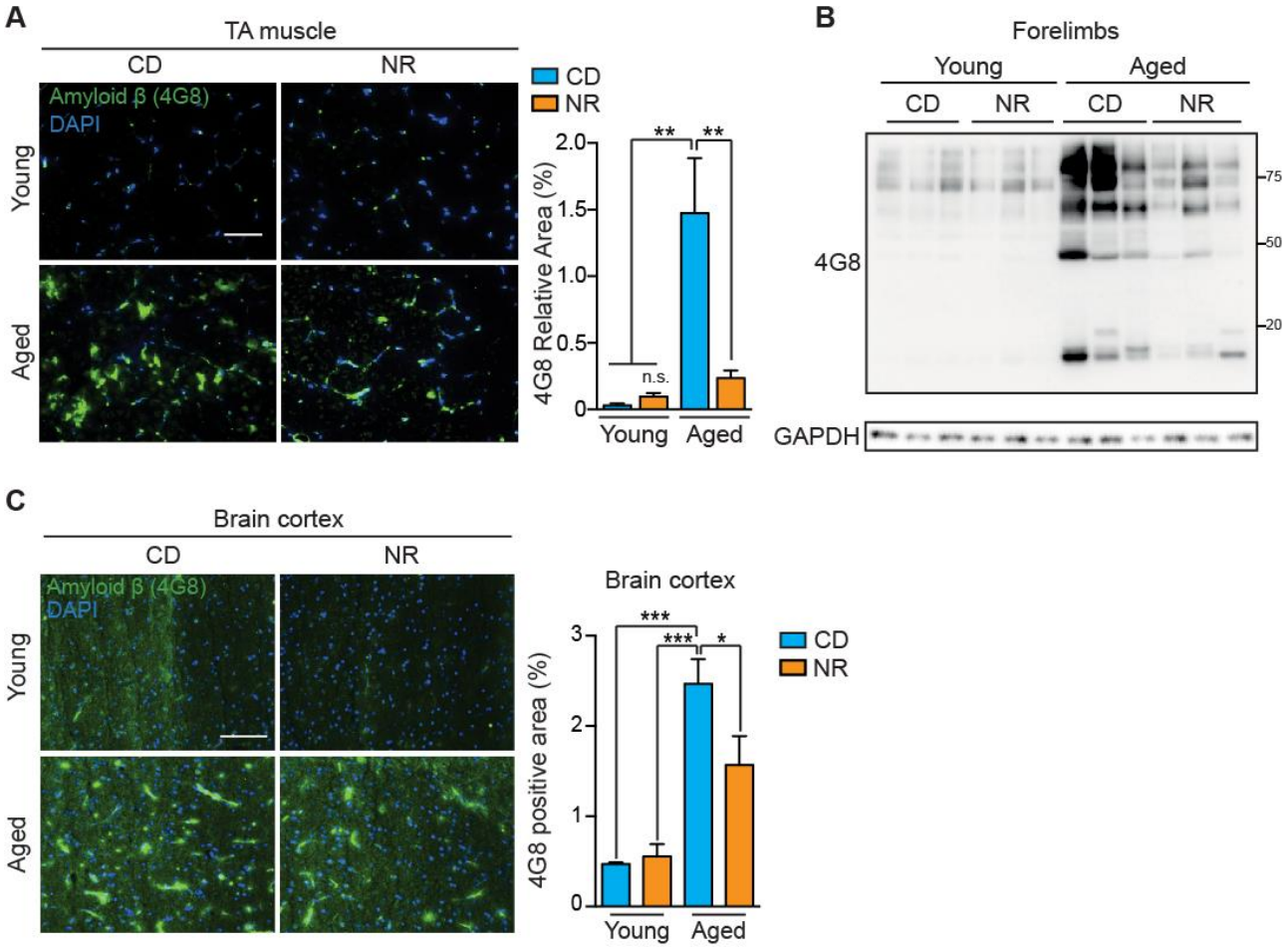

Extended Figure 6. NAD⁺ boosting interventions and their effects on APP and its byproducts in vivo (related to Figure 6). **a**, Representative images and corresponding quantification of immunostainings of 4G8 positive protein deposits in Tibialis anterior (TA) muscles of young or aged male C57BL/6J mice, fed for 8 weeks with chow diet (CD) or chow diet supplemented with NR (400mg/kg/day) (*n* = 5-7 per group). Scale bar, 50µm. **b**, Immunoblot of 4G8 reactive proteins and byproducts from forelimb muscles of the animals in **a** (*n*=3 animals per group). **c**, Representative images and corresponding quantification of immunostainings of 4G8 positive protein deposits in brain of young or aged male C57BL/6J mice, fed for 8 weeks with chow diet (CD) or chow diet supplemented with NR (400mg/kg/day) (*n* = 5-7 per group). Scale bar, 50µm. Values in the figure are mean ± s.e.m. **P*<0.05; ***P*≤0.01; ****P*≤0.001. Differences for two groups were assessed using two-tailed *t* tests (95% confidence interval). For all the individual p values, see the **Excel data source Extended Fig. 6.**

Gene Symbol	Gene ID	Forward	Reverse
act-1	179535	CTACGAACTTCCTGACGGACAAG	CCGGCGGACTCCATACC
pmp-3	179968	GTTCCCGTGTTCATCACTCAT	ACACCGTCGAGAAGCTGTAGA
hsp-6	178873	AGAGCCAAGTTCGAGCAGAT	TCTTGAACAGTGGCTTGCAC
hsp-60	175316	GGAAGCCCAAAGATCACAAA	CAGCCTCCTCATTAGCCTTG
ymel-1	176460	CAAAACCTGATCTCGCTGGG	TTCTCAATGTCGGCTCCAGT
clpp-1	174594	TGATAAGTGCACCAGTGTCCA	TGATTCTGGAGTTCGGGAGA
lonp-1	172966	CGATGATGGCCATTGTGCAG	CGCTTTGAAACATCAATTTCATCCA
sqst-1	178139	GATCCTCCGACCACTCCAAA	TGGAAGTGGTGGAACGATCA
dct-1	181053	GCAAAAGCCGTCTCAAACCC	ACCCACGATTCTGACATACCA
pdr-1	176816	AGCCACCGAGCGATTGATTGC	GTGGCATTTTGGGCATCTTCTTG
pink-1	173918	AAGCACCAGAAATTGCGACG	ACGAGATGGGAGTGCTGGTA
polg-1	174860	TGTTACGGCCGACGAGATAC	TTTCCAGGTTTTCGGCGGTA
hmg-5	177543	CGTCCAAGTGTTCCTCCAAGTG	CTTCGCTTCGTCTGTGTACTTCTTT
sdhb-1	174482	CAGATGCACCAAAGTGTGGC	GTTCGGTGGCGTAGTCATCA
cco-1	172832	GCTCGTCTTGCTGGAGATGATCGTT	GGTCGGCGTCGACTCCCTTG
cox-4	173237	GCCCCAATTCGCGCCAAGGA	AGGTTGGCGGCAGTTCTGGG
nduo-1	2565698	AGCGTCATTTATTGGGAAGAAGAC	AAGCTTGTGCTAATCCCATAAATGT
MTCE.26-1	2565700	GGTTGTGGGACTAGGTGAACA	CAGGGTGCCCCATTGTTCTT
Gapdh	14433	TGTGTCCGTCGTGGATCTGA	CCTGCTTCACCACCTTCTTGAT
B2m	12010	ATGGGAAGCCGAACATACTG	CAGTCTCAGTGGGGGTGAAT
Hspa9	15526	AATGAGAGCGCTCCTTGCTG	CTGTTCCCCAGTGCCAGAAC
Hsp60	15510	GCTGTAGCTGTTACAATGGGG	TGACTTTGCAACAGTGACCC
Yme1l1	27377	AGGGACCTTGGATTATCTGAACT	TGGGATGTATGCCAATGGGAA
Clpp	53895	TGTTGCGGGAACGCATCGTGT	TAGATGGCCAGGCCCGCAGTT
Lonp1	74142	ATGACCGTCCCGGATGTGT	CCTCCACGATCTTGATAAAGCG
Bnip3	12176	CCTGTCGCAGTTGGGTTC	GAAGTGCAGTTCTACCCAGGAG
Sqstm1	18412	GCTGAAGGAAGCTGCCCTAT	TTGGTCTGTAGGAGCCTGGT
Park2	50873	CCGAATCACCTGACGGTTCA	TCTGGCTGCTTCTGAATCCC
Cox5a	12858	GAGCCCAAAATCATTGATGC	TGAGGTCCTGCTTTGTCCTT
Cox2	17709	AACCGAGTCGTTCTGCCAAT	CTAGGGAGGGGACTGCTCAT
Nd1	17716	CAAACACTTATTACAACCCAAGAACA	TCATATTATGGCTATGGGTCAGG
Sdhc	66052	GCTGCGTTCTTGCTGAGACA	ATCTCCTCCTTAGCTGTGGTT

Table S5. List of primers used in *C. elegans* and *M. musculus* (Related to STAR methods).